Structure Changes during the Induction Period of Cold Crystallization of Isotactic Polystyrene Investigated by Infrared and Two-Dimensional Infrared Correlation Spectroscopy

Jianming Zhang,[†] Yongxin Duan,[‡] Deyan Shen,[‡] Shouke Yan,*[,‡] Isao Noda,[§] and Yukihiro Ozaki*[,†]

Department of Chemistry, School of Science and Technology, Kwansei-Gakuin University, Gakuen, Sanda 669-1337, Japan; State Key Laboratory of Polymer Physics & Chemistry, Joint Laboratory of Polymer Science and Materials, Institute of Chemistry, Chinese Academy of Sciences, Beijing 100080, P. R. China; and The Procter & Gamble Company, 8611 Beckett Road, West Chester, Ohio 45069

Received January 13, 2004; Revised Manuscript Received March 1, 2004

ABSTRACT: The structural changes during the induction period of isotactic polystyrene (iPS) cold crystallization were investigated by using infrared (IR) spectroscopy together with 2D correlation analysis. It was found that the ordered orientation of the phenyl ring, local conformation change, and structural formation of 3_1 helix chain of iPS already appear during the induction period. Moreover, careful interpretation of the asynchronous 2D IR spectra generated from the time-dependent spectra enabled us to delineate the structural evolution during the induction period of iPS cold crystallization: Prior to the crystallization of iPS, the amorphous phase changes first, and then the ordering of the phenyl rings of iPS takes place. After that, the polymer chains adjust their local conformations to form the short 3_1 helix structure. The present study has also demonstrated that the generalized 2D IR correlation spectroscopy is powerful in studying small spectral changes in the induction period of polymer crystallization.

1. Introduction

The structural formation during the induction period before crystal growth is one of the most important research topics in polymer physics.[1,2] Although it is still unclear how nucleation proceeds from the amorphous state, with the development of modern light scattering techniques during the past decade, some exciting results have been obtained in this field.[3−12] For example, Imai et al.[3−5] investigated the crystallization process of poly(ethylene terephthalate) (PET) that was annealed just above the glass transition temperature (T_g) by use of small-angle X-ray scattering (SAXS), small-angle neutron scattering (SANS), and depolarized light scattering (DPLS) techniques. Their studies showed that orientation fluctuations or partial parallel ordering of polymer rigid segments actually occur during the induction period of crystallization, which could be understood in analogy with the isotropic-to-nematic transition of liquid crystals presented by Doi et al.[11−14] Using a novel technique of magnetic orientation, Kimura et al.[15] also confirmed that such orientation fluctuations do occur prior to the crystallization of PET. Moreover, Fukao and Miyamoto[16] found the existence of a dynamical transition of amorphous phase from the so-called α process to another relaxation process, named as α′ process, prior to the crystallization of PET. Obviously, these experimental findings based on the scattering techniques are very important to the understanding of the polymer crystallization process. However, there remain a number of open questions regarding the interpretation of the light scattering experiments, which test small density differences between the assumed precursors of the crystal and surrounding melt.

To explore the formation of preordered structures directly in semicrystalline polymer during the induction period at the molecular level, time-resolved IR spectroscopy, which does not require the fully formed three-dimensional crystalline structure to detect the developing molecular order, has also been employed by some researchers.[17−19] It is well documented that IR spectroscopy is a powerful tool for investigating not only the molecular structure but also the conformational order of semicrystalline polymers.[20] Recently, Matsuba et al.[17,18] tried to disclose conformational changes in syndiotactic polystyrene (sPS) and iPS during the induction period with this technique. It is noted that they resorted to the curve-fitting method for analyzing the IR data. In fact, during the induction period of polymer crystallization, variations in vibrational spectra are very small, and this fact may be one of the reasons why only a few vibrational spectroscopy studies on the induction period of polymer crystallization are available in the literature.[17−19] The results of the curve-fitting method heavily depend on the arbitrarily selected parameters, e.g., the peak shape, position, and width. Even if all the procedures for the curve-fitting method are performed intelligently, there always remains some level of ambiguity. If one does not have prior knowledge about the shape, position, and width of bands, the nature of a baseline, and so on, one could reach almost any desired solution.[21] Accordingly, we believe that it is necessary to seek other model-free spectroscopic analysis methods for elucidating the structural changes in the induction period of polymer crystallization.

Generalized two-dimensional (2D) correlation spectroscopy proposed by Noda,[22−24] which is an extension of the original 2D correlation spectroscopy, has become a very powerful and versatile tool for elucidating subtle

† Kwansei-Gakuin University.
‡ Chinese Academy of Sciences.
§ The Procter & Gamble Company.
* To whom all correspondence should be addressed: Fax +81-79-565-9077; e-mail ozaki@ksc.kwansei.ac.jp (y.o.); skyan@iccas.ac.cn (s.y.).

10.1021/ma049910h CCC: $27.50
Published on Web 04/08/2004

spectral changes induced by an external perturbation. It emphasizes spectral features not readily observable in conventional one-dimensional (1D) spectra and probes the specific order of certain events taking place under the influence of a controlled physical variable. The power of the 2D correlation approach results primarily from an enhancement of the spectral resolution that has a physical origin. This effect relies on the dissimilarity among the responses of various submolecular groups absorbing at distinct wavenumbers under a given perturbation. A number of applications of 2D correlation spectroscopy have been reported concerning temperature-, concentration-, and time-dependent spectral changes. Among many features provided by 2D correlation spectroscopy, there are several major advantages of the 2D correlation analysis: (1) It has powerful deconvolution ability for highly overlapped bands. (2) It provides information about inter- and intramolecular interactions by correlating absorption band intensities of different functional groups. (3) The intensity changes of specific sequence occurring during the measurement can be derived from the analysis of the asynchronous spectra. These features are ideally suited for the study of the crystallization process of polymers.

Isotactic polystyrene (iPS) is a semicrystalline polymer characterized by a very slow crystallization rate and low crystallinity (about 30%), making this polymer an ideal subject for an IR study. In our previous study, by monitoring the intensity changes of the characteristic IR bands associated with its crystalline status and 3_1 helix conformation chains, the multiple melting behavior of iPS cold-crystallized at different temperatures was investigated.[25] In the present study, by using IR spectra together with 2D correlation analysis, we explore the structure changes in iPS during the induction period of crystallization. It has been found that the ordering of phenyl rings of iPS, local conformation change, and structural formation of 3_1 helix chain already develop during the induction period. Moreover, the ordering of the phenyl rings emerges prior to the structural formation of short 3_1 helix chain during the induction period and the subsequent crystallization growth process.

2. Experimental Section

2.1. Materials and Preparation Procedures. Powder iPS sample ($M_w \cong 400\,000$, with isotacticity of 90%) was purchased from Scientific Polymer Products, Inc. Amorphous thin films of about 10 μm in thickness were prepared by compression-molding the iPS powder at 250 °C with a pressure of 75 kg/cm^2 and subsequently quenched quickly into ice water at 0 °C. The amorphous thin films thus prepared were dried in a vacuum oven at room temperature for 24 h.

2.2. FTIR Spectroscopy. For the IR experiment of the cold crystallization process, the above-prepared amorphous film was put between two round KBr plates with a spacer of polyimide (ca. 20 μm). The pair of plates were set on a Bruker P/N 21525 series variable temperature cell, which was placed in the sample compartment of a Bruker EQUINOX 55 spectrometer equipped with a DTGS detector. The sample was then heated at 10 °C/min up to 130 °C and annealed for 10 h. IR spectra of the specimens were collected with a 5 °C interval during the annealing process. The spectra were obtained by coadding 32 scans at a 4 cm^{-1} resolution, which took about 30 s.

2.3. DSC Measurement. DSC measurements of the cold-crystallization process at 130 °C were carried out on a Mettler Toledo-822e differential scanning calorimeter with ca. 5 mg of iPS materials sealed in aluminum pans. Nitrogen gas purge with a flux of ca. 50 mL/min was used to prevent oxidative degradation of the samples during heating runs.

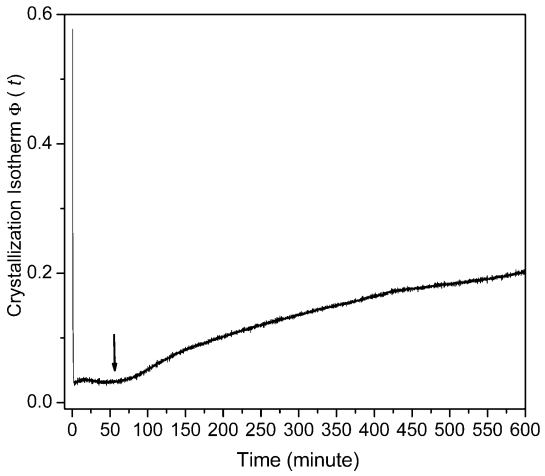

Figure 1. Annealing time dependence of crystallization isotherm at 130 °C for iPS.

2.4. 2D IR Correlation Analysis. Before performing the 2D cross-correlation analysis, the IR spectra were preprocessed to minimize the effect of baseline instabilities and other nonselective effects. The frequency regions of interest (1100−800, 600−520 cm^{-1}) were truncated first and subjected to a linear baseline correction, followed by offsetting to the zero absorbance value. Ten spectra at an equal temperature interval in a certain wavenumber range were selected for the 2D correlation analysis, which was carried out by using the software named "2D Pocha" composed by D. Adachi (Kwansei Gakuin University). The temperature-averaged 1D reference spectra are shown at the side and top of the 2D correlation maps for reference. In the 2D correlation maps, regions without dots indicate positive correlation intensities, while those with dots indicate negative correlation intensities.

3. Results and Discussion

3.1. DSC Measurements. Figure 1 shows the crystallization isotherm $\Phi(t)$ at 130 °C measured by DSC as a function of annealing time t for an amorphous iPS film. It can be seen from the isotherm curve that during the first 60 min, which is referred to as the induction time, neither exotherm nor endotherm is observed. The crystallization has not finished in 600 min, suggesting that the crystallization rate of iPS is very slow.

3.2. Crystallization Characteristics from Infrared Spectra. To elucidate structural changes of iPS during the induction period, we first investigate IR spectral changes of iPS in the whole crystallization process and the assignments of IR bands. Figure 2a,b shows the overall spectra variations during the isothermal cold-crystallization process of iPS at 130 °C for 600 min. It is well established that iPS crystallizes into a 3_1 helix conformation consisting of a regular repetition of trans (T) and gauche (G) conformations of the skeletal C−C bonds.[26] In the present study, we focus on the two regions of the IR spectra that are very sensitive to the structural changes taking place during the crystallization process of iPS. Crystallization- and conformation-sensitive bands of iPS appear in the regions of 1100−800 cm^{-1} (Figure 2a) and 600−520 cm^{-1} (Figure 2b), respectively.[26−28] The band assignments given in the literature are used for the structural analysis.[26−29]

It is well-known that a band at 981 cm^{-1} is a crystallization-sensitive band with an intensity increment in proportion to the degree of crystallinity.[26,27] Bands located at 899, 920, 1052, and 1083 cm^{-1} arise from the 3_1 helix chains, while those located at 840 and 906 cm^{-1} are associated with the amorphous phase of

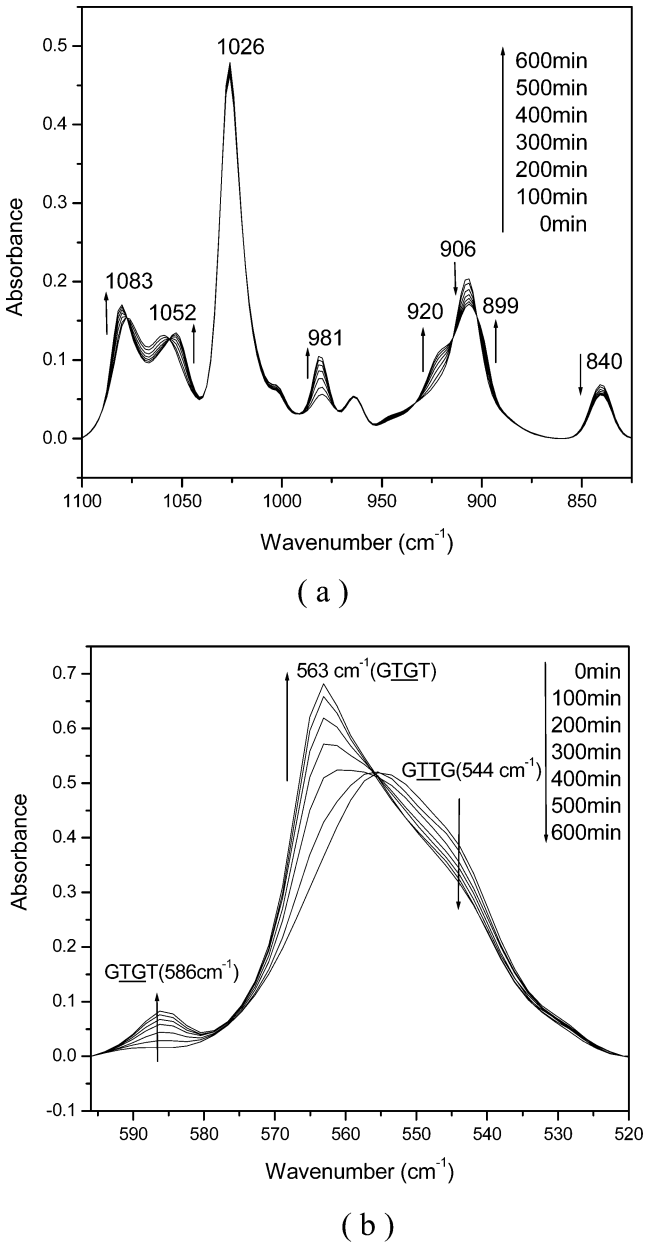

Figure 2. Temporal changes of the IR spectrum in the wavenumber ranges of 800−1100 cm^{-1} (a) and 600−520 cm^{-1} (b) during the crystallization process of iPS at 130 °C. The spectra were collected from 0 to 600 min, with a 100 min interval.

iPS. The appearance of the 3_1 helix bands depends on the sequence length of the helix unit.[28] Kobayashi and co-workers[28,30] introduced a concept of critical sequence length, which depicts the shortest length of the regular sequence with a particular conformation necessary for the appearance of certain 3_1 helix bands. The critical sequence lengths for 3_1 helix bands are different from band to band, e.g., 16 for the 899 cm^{-1} band, 10 for the 920 and 1052 cm^{-1} bands, and 5 for the 1083 cm^{-1} band.[28] The splitting of the 1052 and 1083 cm^{-1} band is mainly related to the regularity of the skeletal chain. The band at 1026 cm^{-1} is due to the localized vibrational mode associated with the C−H in-plane bending of the phenyl ring. This band is usually chosen as an internal standard since its intensity is not affected by its crystalline status.[31] From Figure 2a, it can be clearly seen that the intensities of bands at 981, 899, 920, 1052, and 1083 cm^{-1} associated with the crystalline and 3_1 helix chains of iPS increase with time, while those at 840 and 906 cm^{-1} due to its amorphous counterpart decrease. This trend unambiguously indicates the progress of the crystallization process. IR bands in the region of 600−520 cm^{-1} (Figure 2b) are attributed to the out-of-plane modes of phenyl groups.[18,28] They reflect the local conformation rather than the sequential array of polymer chains. At least three obvious components can be observed in Figure 2b. A band at 586 cm^{-1} and one around 563 cm^{-1} have been assigned to the G*TG*T conformation, and a band around 544 cm^{-1} is assigned to the G*TT*G one.[18] Here, T and G are trans and gauche conformations, respectively, and the two middle italic letters indicate the conformations around the C−C bonds on the both sides of the carbon atom bonded to the phenyl group. These bands are observed in both amorphous and crystalline spectra of iPS, as seen in Figure 2b.

Figure 3 shows IR spectra in the regions of 1100−800 cm^{-1} (Figure 3a) and 600−520 cm^{-1} (Figure 3b) collected in the induction period of cold crystallization of iPS. To demonstrate the spectral differences among the spectra measured at different times, six spectra with a 10 min interval are overlaid in Figure 3a,b. It can be seen from Figure 3a that the differences among these spectra are very small. It is not easy to detect the changes in bands associated with the local molecular conformation and 3_1 helix chain conformation of iPS from the 1D IR spectra of Figure 3a,b. Bands at 899, 920, 1052, and 1083 cm^{-1} are heavily overlapped with each other. However, it is noted in Figure 3a that a relatively obvious change can be recognized for the 981 cm^{-1} band. As mentioned above, usually this band is attributed to a crystallization-sensitive band. If this assignment is correct, it means that no induction period should exist when iPS crystallizes at 130 °C, which obviously is in contradiction with the DSC results. Moreover, we notice that this band also appears even in the amorphous state. Therefore, it cannot be a true crystallization band. Kobayashi et al.[29] also found that the intensity of this band does not increase through the gelation process but remains at a level as low as in the glassy state. By investigating the intensity of the 983 cm^{-1} band for the isotactic copolymer of styrene and ring-deuterated styrene, as well as the blend of iPS and iPS-r-d5, they obtained the direct evidence that the 981 cm^{-1} band is in no relationship with either the inter- or intramolecular interactions. At the same time, considering that the 981 cm^{-1} band is assumed to be the ring C−H out-of-plane mode with no relation to a vibrational mode of the main chain, they concluded that this kind of crystallization-sensitivity band arises from the ordering of phenyl rings. Such assignment also gives a rational explanation for our spectral data obtained during the induction period of iPS. That is, during the induction period well before the full crystallization, the ordering of the phenyl rings of iPS already develops.

3.3. Two-Dimensional Correlation Analysis. 3.3.1. The 1100−800 cm^{-1} Region. The synchronous 2D spectrum $\Phi(\nu_1,\nu_2)$ in the range 1100−800 cm^{-1} generated from the time-dependent spectra in Figure 3a is displayed in Figure 4a. For comparison, the corresponding synchronous spectrum calculated from the data recorded after the induction period (from 100 to 600 min) is given in Figure 4b. Unexpectedly, the patterns of Figure 4a,b are surprisingly similar to each other. In both 2D spectra, it can be seen that highly overlapped

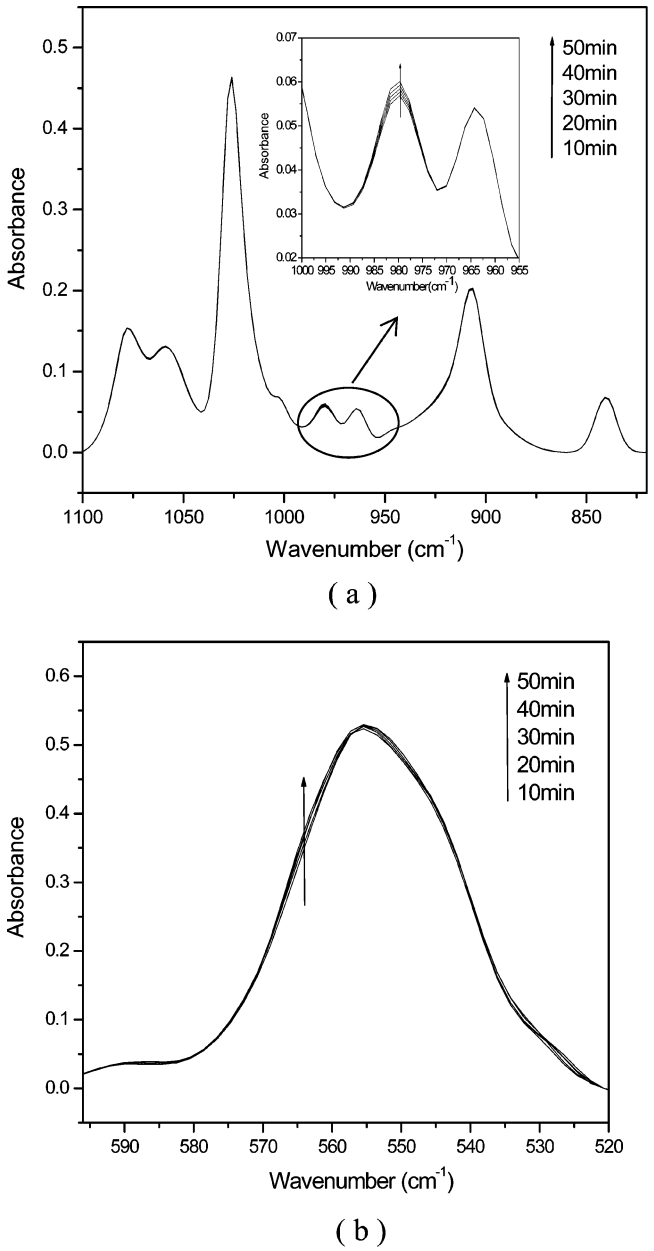

Figure 3. Temporal changes of an IR spectrum in the wavenumber ranges of 800−1100 cm^{-1} (a) and 600−520 cm^{-1} (b) during the crystallization process of iPS at 130 °C. The spectra were recorded from 10 to 50 min, with a 10 min interval.

peaks in the ranges 950−870 and 1100−1040 cm^{-1} are deconvoluted effectively by spreading the peaks along the second spectral dimension. In the range 950−870 cm^{-1}, three autopeaks can be detected unambiguously. The appearance of these peaks is consistent with the well-known assignments: the 899 and 920 cm^{-1} bands are due to the 3_1 helix structure, and the 906 cm^{-1} band is associated with the amorphous state of iPS. In the range 1100−1040 cm^{-1}, two autopeaks at 1052 and 1083 cm^{-1} associated with the appearance of the 3_1 helix structure are developed. In this way, compared with 1D spectra in Figure 3a, the changes in the bands at 899, 920, 1052, and 1083 cm^{-1} due to the 3_1 helical chain structure can be detected clearly in the synchronous 2D spectrum of iPS during the induction period and the crystallization process. The result further indicates that the formation of the 3_1 helical chain conformation proceeds even during the induction period before the

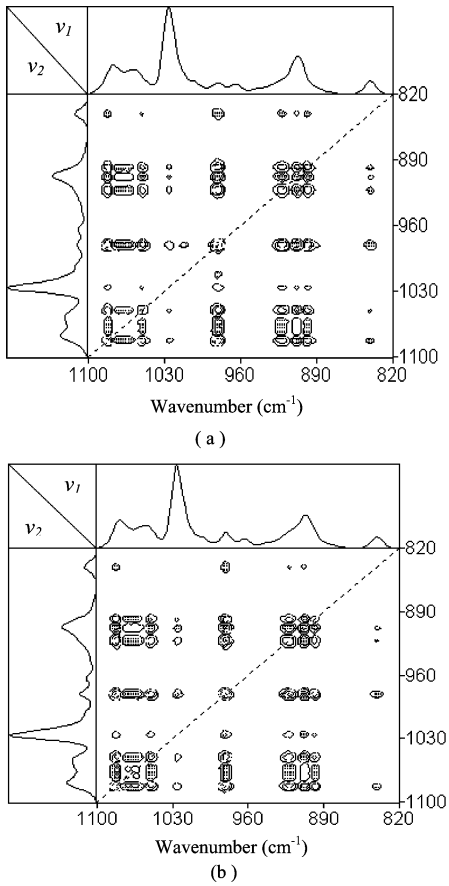

Figure 4. Synchronous correlation spectra of iPS, in the wavenumber region of 1100−800 cm^{-1}, calculated from the spectra obtained during annealing at 130 °C: (a) spectra obtained from 10 to 50 min; (b) those from 100 to 600 min.

onset of crystallization. An autopeak corresponding to the 981 cm^{-1} band in Figure 4a means that the ordered alignment of phenyl rings of iPS starts during the induction period, which is in agreement with the conclusion disclosed from the previously shown 1D IR spectrum.

According to the sign of cross-peaks in Figure 4a, the intensities of the bands at 899, 920, 1052, and 1083 cm^{-1} due to the 3_1 helix structure and that of the band at 981 cm^{-1} due to the order orientation of phenyl ring of iPS increase during the induction period, while those of the bands at 906 and 840 cm^{-1} associated with the amorphous state decrease. As mentioned above, the 1026 cm^{-1} band is usually chosen as an internal standard for calculating the crystallization degree since it is believed that the intensity is not greatly affected by crystallization. However, in the synchronous spectrum, the 1026 cm^{-1} band also develops positive cross-peaks with the bands at 899, 920, 1052, and 1083 cm^{-1}, which are sensitive to the 3_1 helix structure, and a negative cross-peak with the amorphous band at 906 cm^{-1}. This result indicates that the intensity of the 1026 cm^{-1} band also slightly increases during the induction period, although its intensity change is very small.

Figure 5a,b shows the asynchronous spectra $\Psi(\nu_1,\nu_2)$ of iPS corresponding to the synchronous spectra in Figure 4a,b, respectively. An asynchronous spectrum represents sequential or successive changes of spectral intensities measured at ν_1 and ν_2. According to Noda's rules,[22,23] the sign of an asynchronous cross-peak becomes positive if the intensity change at ν_1 occurs

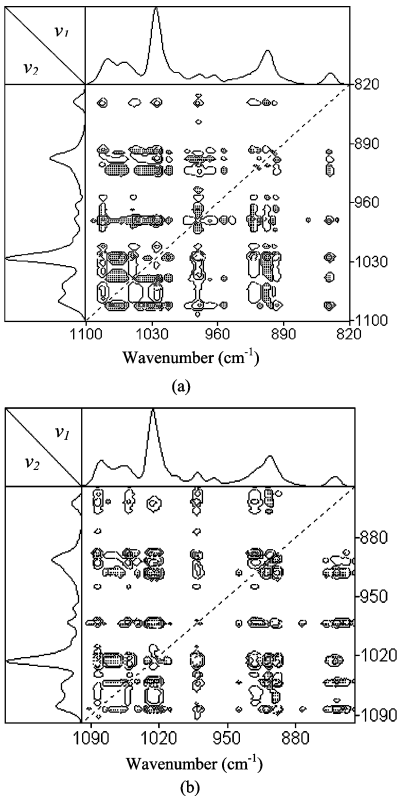

Figure 5. Asynchronous correlation spectra of iPS, in the wavenumber region of 1100−800 cm^{-1}, calculated from the spectra obtained during annealing at 130 °C: (a) spectra recorded from 10 to 50 min; (b) those from 100 to 600 min.

predominantly before ν_2 in the sequential order of t. It becomes negative, on the other hand, if the change occurs after ν_2. This rule is, however, reversed if the corresponding synchronous intensity becomes negative, i.e., $\Phi(\nu_1,\nu_2) < 0$. On the basis of this unique feature of asynchronous spectra, we naturally expected to obtain more information about the induction period of iPS crystallization from the asynchronous spectra, especially about the order of structure changes. Compared with the synchronous spectra in Figure 4, the corresponding asynchronous spectra in Figure 5 are more strongly influenced by fine details of spectral fluctuations. There are some unexpected cross-peaks and irregular patterns appearing in Figure 5. This result reveals the high sensitivity of asynchronous 2D correlation spectra to fluctuations of the experimental spectra. However, of great importance is the fact that the asynchronous spectra can reflect even small intensity distortions in the original data set. Recently, by studying polymer blends with 2D IR spectroscopy, Huang et al.[32,33] pointed out that some features generated in a 2D asynchronous map may be results of small frequency shifts or bandwidth changes rather than those of revealing underlying new bands that are difficult to detect. In the present case, spectral pretreatment has been done for reducing effects of some spectral distortions, such as random noise and baseline fluctuation. Nevertheless, other effects such as frequency shifts and bandwidth variations cannot be removed from the experimental spectra, so caution must be taken during the interpretation of asynchronous spectra. For example, the critical sequence lengths for the 3_1 helix bands in the spectrum are 16 for the 899 cm^{-1} band and 10 for the 920 cm^{-1} band. Consequently, the 920 cm^{-1} band should appear prior to the 899 cm^{-1} band during the crystallization process. However, from $\Phi(920, 899) > 0$ and $\Psi(920, 899) < 0$ presented respectively in Figure 4b and Figure 5b, according to the rule, the intensity change of the 899 cm^{-1} band should occur prior to that of the 920 cm^{-1} band. Obviously, this apparent sequence is not rational. In Figure 5b, it is noticed that a so-called butterfly pattern appears in the overlap range of 950−870 cm^{-1} in which three peaks are enclosed as mentioned above. Usually, such a pattern in an asynchronous spectrum is attributed to a very small peak shift (even 0.01 cm^{-1}) during the intensity change.[33] Obviously, in such case, it is not suitable to interpret the cross-peaks in the region of 950−870 cm^{-1} with the conventional Noda's rule. In Figure 5a, the pattern of cross-peaks among the two overlapping regions (950−870 and 1100−1040 cm^{-1}) is also complicated by some spectral perturbation.

Although there is some interference in the overlapped spectra ranges, some valuable information still can be obtained from several well-separated cross-peaks in Figures 4a and 5a. First, $\Phi(1083, 840)$, $\Phi(1052, 840)$, and $\Phi(981, 840) < 0$ in the synchronous spectrum of Figure 4a, and $\Psi(1083, 840)$, $\Psi(1052, 840)$, and $\Psi(981, 840) > 0$ in the corresponding asynchronous spectrum of Figure 5a, indicate that the amorphous band at 840 cm^{-1} changes prior to the bands at 1083 and 1052 cm^{-1} associated with the short 3_1 helix chain conformation and the band at 981 cm^{-1} due to the ordered orientation of the phenyl rings of iPS. It means that, prior to the structure ordering of the molecular chain or the phenyl rings of iPS during the induction period, the amorphous phase changes first. Here, we cannot provide more practical information on what changes occur in the amorphous phase before the structure ordering in the induction period. However, this result adds support to other researchers' findings and ideas: Dynamical transition or density fluctuation of amorphous phase also appears prior to polymer crystallization.[16,34] Second, we find $\Phi(1083, 981) > 0$ and $\Phi(1052, 981) > 0$ in Figure 4a and $\Psi(1083, 981) < 0$ and $\Psi(1052, 981) < 0$ in Figure 5a, indicating that the intensity change of the 981 cm^{-1} band occurs before the bands at 1083 and 1052 cm^{-1}. In other words, the ordering of phenyl rings of iPS takes place prior to the structural formation of short 3_1 helix chains during the induction period. During the iPS crystallization process, the same sequential order of these bands also can be concluded from the 2D spectra in Figures 4b and 5b.

3.3.2. The 600−520 cm^{-1} Region. Figure 6a shows the synchronous 2D IR spectrum in the range 600−520 cm^{-1} calculated from the spectra measured during the induction period (Figure 3b) of iPS. The corresponding spectrum generated from the spectra recorded during the crystallization process of iPS is also presented in Figure 6b. Unlike the case for the range 1100−800 cm^{-1}, there is an obvious difference between the synchronous 2D IR spectrum for the induction period and that for the crystallization process of iPS. In Figure 6a, six components (527, 535, 544, 553, 564, and 586 cm^{-1}) can be detected in the range 600−520 cm^{-1}. However, in Figure 6b, only three components (544, 564, and 586 cm^{-1}) are developed. The reason for this difference is that, during the crystallization process of iPS, the intensities of the bands associated with G*TG*T and G*TG*T conformation change greatly as revealed in the 1D spectrum (Figure 2b), and thus some components with a small intensity change in this range are over-

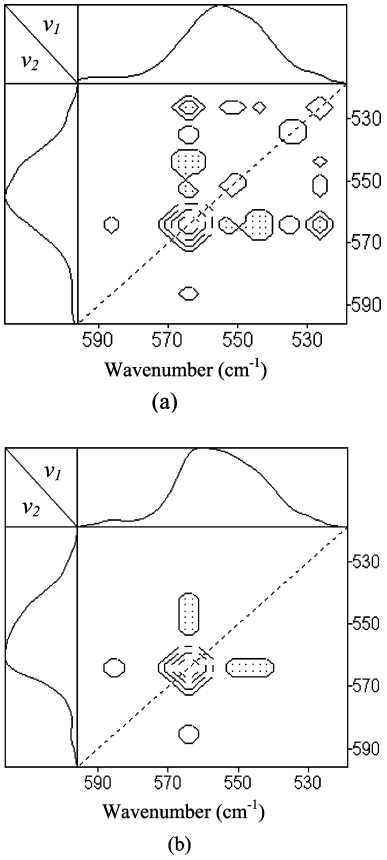

Figure 6. Synchronous correlation spectra of iPS, in the wavenumber region 600−520 cm^{-1}, calculated from the spectra obtained during annealing at 130 °C: (a) spectra recorded from 0 to 50 min; (b) those from 100 to 600 min.

whelmed in the synchronous 2D IR spectrum. During the induction period, the situation is very different. As indicated in the 1D spectrum (Figure 3b), the change is very small for all the components in this spectral range, and thus all the components are disclosed effectively in the synchronous 2D IR spectrum. To follow the conformational change during the induction period, Matsuba et al.[18] decomposed the spectra in the region of 600−500 cm^{-1} into four components by assuming a Lorentzian shape for each band. From our synchronous 2D spectrum (Figure 6a), in the induction period of iPS, it seems that at least six components should be included.

Figure 7 shows (a) the difference spectrum obtained by subtracting the IR spectrum of iPS measured at 0 min from that measured at 50 min and (b−d) the second derivative of the spectra measured at 0, 50, and 600 min during the isotherm crystallization process of iPS at 130 °C, respectively. Obviously, the band at 535 cm^{-1} corresponds to "concave upward" lobe in the difference spectrum and the second-derivative spectra. Therefore, the 535 cm^{-1} band disclosed by the synchronous 2D spectrum (Figure 6a) probably is not a real band. The bands at 527, 544, and 586 cm^{-1} can be revealed unambiguously by the difference spectrum and the second-derivative spectra. From the second-derivative spectra in Figure 7, it is found that there is a large peak shift for the band around 563 cm^{-1} during the crystallization process. This band shifts from 556 to 563 cm^{-1} after amorphous iPS crystallizes at 130 °C for 600 min. On the other hand, from the difference spectrum in Figure 7, it seems that two bands at 553 and 564 cm^{-1} are enclosed in this peak, which is consistent with the

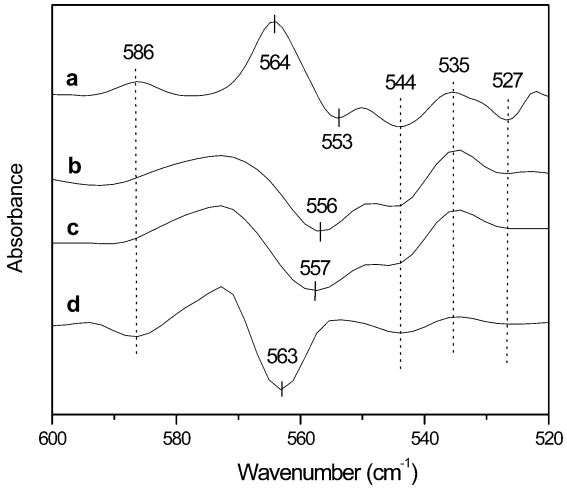

Figure 7. Difference spectrum obtained by the subtraction of the IR spectrum of iPS measured at 0 min from that measured at 50 min (a), second derivative of spectra measured at 0 min (b), 50 min (c), and 600 min (d) during the isotherm crystallization process of iPS at 130 °C.

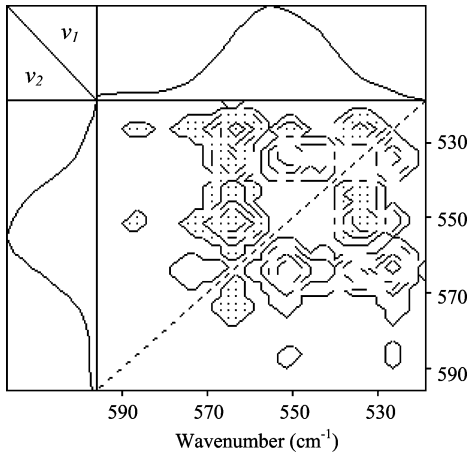

Figure 8. Asynchronous correlation spectrum of iPS, in the wavenumber region of 600−520 cm^{-1}, calculated from the spectra obtained from 0 to 50 min during annealing at 130 °C.

result of synchronous 2D spectrum in Figure 6a. Therefore, it is speculated that at least five components should be enclosed in the region of 600−520 cm^{-1}.

The irregular patterns of the asynchronous 2D IR spectrum corresponding to Figure 6a (shown in Figure 8) indicate that small band shifts or band broadening for those associated with conformational change are present during the induction period of iPS. The main point we wish to make here is that the change in the local conformation of iPS during the induction period does exist as revealed from the synchronous 2D IR spectrum in this spectral range of 600−520 cm^{-1}. However, because it is difficult to ensure the accurate detection of components in this region, and the existence of band shifts or broadening for the bands associated with the conformation change, we believe that a simple curve-fitting method is not suitable for exploring such small differences in the induction period of iPS. In Figure 6a, we observe $\Phi(586, 564) > 0$ and $\Phi(564, 544) < 0$, which indicate that the intensities of the 586 and 564 cm^{-1} bands associated with the G*TG*T conformation of iPS increase, while the intensity of the 544 cm^{-1} band due to the G*TT*G decreases during the induction period of iPS. This trend of conformational change is the same

as that during the crystallization process of iPS as shown in the 1D and 2D spectra (Figures 2b and 6b).

3.4. Conclusion. The present study has shown that the generalized 2D IR correlation spectroscopy is powerful in studying the structural changes during the induction period of iPS cold crystallization. It has been found that the structural change of iPS during the induction period, such as the ordered orientation of the phenyl ring, local conformational changes, and the formation of a short 3_1 helix chain, can be disclosed unambiguously from the synchronous 2D IR spectra. Moreover, the detailed analysis of the asynchronous 2D IR spectra has revealed the sequence of structural evolution during the induction period of iPS crystallization. That is, prior to the crystallization of iPS, the amorphous phase changes first, and then ordered orientation of the phenyl rings of iPS takes place. After that, the polymer chains adjust their local conformations to form short 3_1 helix chains.

Acknowledgment. Jianming Zhang thanks the Japan Society for the Promotion of Science (JSPS) for financial support. Also, the financial support of the National Natural Science Foundation of China (No. 20374056) and the CAS hundred talents program are gratefully acknowledged.

References and Notes

(1) Katayama, K.; Amano, T.; Nakamura, K. *Kolloid Z. Z. Polym.* **1968**, *126*, 125.
(2) Strobl, G. R. *The Physics of Polymers*; Springer-Verlag: Berlin, 1996.
(3) Imai, M.; Mori, K.; Mizukami, T.; Kaji, K.; Kanaya, T. *Polymer* **1992**, *33*, 4451.
(4) Imai, M.; Mori, K.; Mizukami, T.; Kaji, K.; Kanaya, T. *Polymer* **1992**, *33*, 4457.
(5) Imai, M.; Kaji, K.; Kanaya, T.; Sakai, Y. *Phys. Rev. B* **1995**, *52*, 12696.
(6) Strobl, G. R. In *Trends in Non-Crystalline Solids*; Conde, A., Conde, C. F., Millán, M., Eds.; World Scientific: Singapore, 1992; p 37.
(7) Cakmak, M.; Teitge, A.; Zachmann, H. G.; White, J. L. *J. Polym. Sci., Part B: Polym. Phys.* **1993**, *31*, 371.
(8) Terrill, N. J.; Fairclough, P. A.; Town-Andrews, E.; Komanschek, B. U.; Young, R. J.; Ryan, A. J. *Polymer* **1998**, *39*, 2381.
(9) Ezquerra, T. A.; López-Cabarcos, E.; Hsiao, B. S.; Baltà-Callaeja, F. J. *Phys. Rev. E* **1996**, *54*, 989.
(10) Kaji, K.; Imai, M. Dynamics of Structure Formation during the Induction Period of Polymer Crystallization. In *The Physics of Complex Liquids*; Yonezawa, F., Tsuji, K., Kaji, K., Doi, M., Fujiwara, T., Eds.; World Scientific: Singapore, 1998.
(11) Doi, M.; Edwards, S. F. *The Theory of Polymer Dynamics*; Clarendon Press: Oxford, England, 1986; Chapter 10.
(12) Shimada, T.; Doi, M.; Okano, K. *J. Chem. Phys.* **1988**, *88*, 2815.
(13) Doi, M.; Shimada, T.; Okano, K. *J. Chem. Phys.* **1988**, *88*, 4070.
(14) Shimada, T.; Doi, M.; Okano, K. *J. Chem. Phys.* **1988**, *88*, 7181.
(15) Kimura, T.; Ezure, H.; Tanaka, S.; Ito, E. *J. Polym. Sci., Part B* **1998**, *36*, 1227.
(16) Fukao, K.; Miyamoto, Y. *Phys. Rev. Lett.* **1997**, *79*, 4613.
(17) Matsuba, G.; Kaji, K.; Nishida, K.; Kanaya, T.; Imai, M. *Macromolecules* **1999**, *32*, 8932.
(18) Matsuba, G.; Kaji, K.; Nishida, K.; Kanaya, T.; Imai, M. *Polym. J.* **1999**, *31*, 722.
(19) Jiang, Y.; Gu, Q.; Li, L.; Shen, D, Y.; Jin, X. G.; Chan, C. M. *Polymer* **2003**, *44*, 3509.
(20) Chalmers, J. M.; Hannah, R. W.; Mayo, D. W. Spectra-structure correlations: Polymer spectra. In *Handbook of Vibrational Spectroscopy*; Chalmers, J. M., Griffiths, P. R., Eds.; John Wiley & Sons Ltd.: London, UK, 2002; Vol. 4.
(21) Skrovanek, D. J.; Painter, P. C.; Coleman, M. M. *Macromolecules* **1986**, *19*, 699.
(22) Noda, I. *Appl. Spectrosc.* **1993**, *47*, 1329.
(23) Noda, I. *Appl. Spectrosc.* **2000**, *54*, 994.
(24) Noda, I.; Dowrey, A. E.; Marcott, C.; Story, G. M.; Ozaki, Y. *Appl. Spectrosc.* **2000**, *54*, 236.
(25) Duan, Y. X.; Zhang, J. M.; Shen, D. Y.; Yan, S. K. *Macromolecules* **2003**, *36*, 4847.
(26) Kobayashi, M.; Tsumura, K.; Tadokoro, H. *J. Polym. Sci.* **1968**, *6*, 1493.
(27) Painter, P. C.; Koenig, J. L. *J. Polym. Sci., Part B: Polym. Phys.* **1982**, *2*, 2277.
(28) Kobayashi, M.; Nakaoki, T.; Ishihara, N. *Macromolecules* **1990**, *23*, 78.
(29) Nakaoki, T.; Katagiri, C.; Kobayashi, M. *Macromolecules* **2002**, *35*, 7708.
(30) Kobayashi, M.; Akita, K.; Tadokoro, H. *Makromol. Chem.* **1968**, *118*, 324.
(31) Kimura, T.; Ezure, H.; Tanaka, S.; Ito, E. *J. Polym. Sci., Part B: Polym. Phys.* **1998**, *36*, 1227.
(32) Huang, H.; Malkov, S.; Coleman, M.; Painter, P. *Macromolecules* **2003**, *36*, 8148.
(33) Huang, H.; Malkov, S.; Coleman, M.; Painter, P. *Macromolecules* **2003**, *36*, 8156.
(34) Olmsted, P. D.; Poon, W. C. K.; McLeish, T. C. B.; Terrill, N. J.; Ryan, A. J. *Phys. Rev. Lett.* **1998**, *81*, 373.

MA049910H